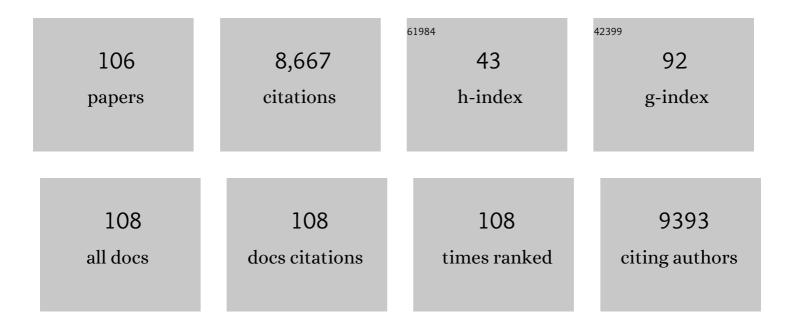
## Andreas Heyden

List of Publications by Year in descending order

Source: https://exaly.com/author-pdf/4760322/publications.pdf Version: 2024-02-01



#	Article	IF	CITATIONS
1	Advances in methods and algorithms in a modern quantum chemistry program package. Physical Chemistry Chemical Physics, 2006, 8, 3172-3191.	2.8	2,597
2	Efficient methods for finding transition states in chemical reactions: Comparison of improved dimer method and partitioned rational function optimization method. Journal of Chemical Physics, 2005, 123, 224101.	3.0	662
3	A growing string method for determining transition states: Comparison to the nudged elastic band and string methods. Journal of Chemical Physics, 2004, 120, 7877-7886.	3.0	293
4	Upcycling Single-Use Polyethylene into High-Quality Liquid Products. ACS Central Science, 2019, 5, 1795-1803.	11.3	283
5	Analysis of Kinetics and Reaction Pathways in the Aqueous-Phase Hydrogenation of Levulinic Acid To Form Î <sup>3</sup> -Valerolactone over Ru/C. ACS Catalysis, 2014, 4, 1171-1181.	11.2	265
6	Catalytic upcycling of high-density polyethylene via a processive mechanism. Nature Catalysis, 2020, 3, 893-901.	34.4	262
7	Electronic Properties of Bimetallic Metal–Organic Frameworks (MOFs): Tailoring the Density of Electronic States through MOF Modularity. Journal of the American Chemical Society, 2017, 139, 5201-5209.	13.7	178
8	Comprehensive DFT Study of Nitrous Oxide Decomposition over Fe-ZSM-5â€. Journal of Physical Chemistry B, 2005, 109, 1857-1873.	2.6	176
9	Adaptive Partitioning in Combined Quantum Mechanical and Molecular Mechanical Calculations of Potential Energy Functions for Multiscale Simulations. Journal of Physical Chemistry B, 2007, 111, 2231-2241.	2.6	172
10	Synthesis and characterization of Mo-doped SrFeO3â^î^ as cathode materials for solid oxide fuel cells. Journal of Power Sources, 2012, 202, 63-69.	7.8	147
11	On the importance of metal–oxide interface sites for the water–gas shift reaction over Pt/CeO2 catalysts. Journal of Catalysis, 2014, 309, 314-324.	6.2	142
12	Progress in Accurate Chemical Kinetic Modeling, Simulations, and Parameter Estimation for Heterogeneous Catalysis. ACS Catalysis, 2019, 9, 6624-6647.	11.2	134
13	Î2-O-4 Bond Cleavage Mechanism for Lignin Model Compounds over Pd Catalysts Identified by Combination of First-Principles Calculations and Experiments. ACS Catalysis, 2016, 6, 5589-5598.	11.2	116
14	Theoretical Investigation of the Reaction Mechanism of the Guaiacol Hydrogenation over a Pt(111) Catalyst. ACS Catalysis, 2015, 5, 2423-2435.	11.2	111
15	Liquid-Phase Modeling in Heterogeneous Catalysis. ACS Catalysis, 2018, 8, 2188-2194.	11.2	101
16	Theoretical investigation of the reaction mechanism of the hydrodeoxygenation of guaiacol over a Ru(0 0 0 1) model surface. Journal of Catalysis, 2015, 321, 39-50.	6.2	100
17	Conservative Algorithm for an Adaptive Change of Resolution in Mixed Atomistic/Coarse-Grained Multiscale Simulations. Journal of Chemical Theory and Computation, 2008, 4, 217-221.	5.3	94
18	Active Sites in Copper-Based Metal–Organic Frameworks: Understanding Substrate Dynamics, Redox Processes, and Valence-Band Structure. Journal of Physical Chemistry C, 2015, 119, 27457-27466.	3.1	87

#	Article	IF	CITATIONS
19	Microkinetic modeling of the decarboxylation and decarbonylation of propanoic acid over Pd(111) model surfaces based on parameters obtained from first principles. Journal of Catalysis, 2013, 305, 56-66.	6.2	81
20	A Reaction Mechanism for the Nitrous Oxide Decomposition on Binuclear Oxygen Bridged Iron Sites in Fe-ZSM-5. Journal of Physical Chemistry C, 2007, 111, 2092-2101.	3.1	80
21	Water-Gas Shift Activity of Atomically Dispersed Cationic Platinum versus Metallic Platinum Clusters on Titania Supports. ACS Catalysis, 2017, 7, 301-309.	11.2	78
22	Nitrous Oxide Decomposition over Fe-ZSM-5 in the Presence of Nitric Oxide: A Comprehensive DFT Study. Journal of Physical Chemistry B, 2006, 110, 17096-17114.	2.6	77
23	Origin of the unique activity of Pt/TiO2 catalysts for the water–gas shift reaction. Journal of Catalysis, 2013, 306, 78-90.	6.2	76
24	Prediction of Adsorption Energies for Chemical Species on Metal Catalyst Surfaces Using Machine Learning. Journal of Physical Chemistry C, 2018, 122, 28142-28150.	3.1	74
25	Adsorbate-Induced Changes in the Surface Composition of Bimetallic Clusters: Ptâ^'Au on TiO <sub>2</sub> (110). Journal of Physical Chemistry C, 2010, 114, 21652-21663.	3.1	70
26	Theoretical Investigation of the Reaction Mechanism of the Decarboxylation and Decarbonylation of Propanoic Acid on Pd(111) Model Surfaces. Journal of Physical Chemistry C, 2012, 116, 14328-14341.	3.1	70
27	Kinetic modeling of nitrous oxide decomposition on Fe-ZSM-5 based on parameters obtained from first-principles calculations. Journal of Catalysis, 2005, 233, 26-35.	6.2	68
28	Theoretical Investigation of H <sub>2</sub> Oxidation on the Sr <sub>2</sub> Fe <sub>1.5</sub> Mo <sub>0.5</sub> O <sub>6</sub> (001) Perovskite Surface under Anodic Solid Oxide Fuel Cell Conditions. Journal of the American Chemical Society, 2014, 136, 8374-8386.	13.7	68
29	Toward rational design of stable, supported metal catalysts for aqueous-phase processing: Insights from the hydrogenation of levulinic acid. Journal of Catalysis, 2015, 329, 10-21.	6.2	65
30	Theoretical Investigation of the Hydrodeoxygenation of Levulinic Acid to $\hat{I}^3$ -Valerolactone over Ru(0001). ACS Catalysis, 2017, 7, 215-228.	11.2	65
31	Microkinetic modeling of nitrous oxide decomposition on dinuclear oxygen bridged iron sites in Fe-ZSM-5. Journal of Catalysis, 2007, 248, 213-225.	6.2	63
32	Size-Controlled Nanoparticles Embedded in a Mesoporous Architecture Leading to Efficient and Selective Hydrogenolysis of Polyolefins. Journal of the American Chemical Society, 2022, 144, 5323-5334.	13.7	60
33	Modeling the noble metal/TiO2 (110) interface with hybrid DFT functionals: A periodic electrostatic embedded cluster model study. Journal of Chemical Physics, 2010, 133, 164703.	3.0	59
34	Water–Gas Shift Catalysis at Corner Atoms of Pt Clusters in Contact with a TiO <sub>2</sub> (110) Support Surface. ACS Catalysis, 2014, 4, 3654-3662.	11.2	56
35	Uncertainty Quantification Framework Applied to the Water–Gas Shift Reaction over Pt-Based Catalysts. Journal of Physical Chemistry C, 2016, 120, 10328-10339.	3.1	56
36	Controlling reaction pathways of selective C–O bond cleavage of glycerol. Nature Communications, 2018, 9, 4612.	12.8	54

#	Article	IF	CITATIONS
37	Ni modified ceramic anodes for solid oxide fuel cells. Journal of Power Sources, 2012, 201, 43-48.	7.8	52
38	Solvent effects on the hydrodeoxygenation of propanoic acid over Pd(111) model surfaces. Green Chemistry, 2014, 16, 605-616.	9.0	51
39	Identifying Active Sites of the Water–Gas Shift Reaction over Titania Supported Platinum Catalysts under Uncertainty. ACS Catalysis, 2018, 8, 3990-3998.	11.2	49
40	Understanding the Nature and Activity of Supported Platinum Catalysts for the Water–Gas Shift Reaction: From Metallic Nanoclusters to Alkali-Stabilized Single-Atom Cations. ACS Catalysis, 2019, 9, 7721-7740.	11.2	48
41	New Implicit Solvation Scheme for Solid Surfaces. Journal of Physical Chemistry C, 2012, 116, 22458-22462.	3.1	47
42	On the Importance of the Associative Carboxyl Mechanism for the Water-Gas Shift Reaction at Pt/CeO <sub>2</sub> Interface Sites. Journal of Physical Chemistry C, 2014, 118, 6314-6323.	3.1	47
43	Combined DFT and Microkinetic Modeling Study of Hydrogen Oxidation at the Ni/YSZ Anode of Solid Oxide Fuel Cells. Journal of Physical Chemistry Letters, 2012, 3, 2767-2772.	4.6	46
44	Theoretical investigation of the decarboxylation and decarbonylation mechanism of propanoic acid over a Ru(0 0 0 1) model surface. Journal of Catalysis, 2015, 324, 14-24.	6.2	45
45	Nature of Pt <sub><i>n</i></sub> /TiO <sub>2</sub> (110) Interface under Water-Gas Shift Reaction Conditions: A Constrained ab Initio Thermodynamics Study. Journal of Physical Chemistry C, 2011, 115, 19246-19259.	3.1	44
46	Hybrid Quantum Mechanics/Molecular Mechanics Solvation Scheme for Computing Free Energies of Reactions at Metal–Water Interfaces. Journal of Chemical Theory and Computation, 2014, 10, 3354-3368.	5.3	42
47	Investigation of solvent effects in the hydrodeoxygenation of levulinic acid to Î <sup>3</sup> -valerolactone over Ru catalysts. Journal of Catalysis, 2019, 379, 164-179.	6.2	42
48	Solvation Effects in the Hydrodeoxygenation of Propanoic Acid over a Model Pd(211) Catalyst. Journal of Physical Chemistry C, 2016, 120, 2724-2736.	3.1	40
49	Solvent effects in the liquid phase hydrodeoxygenation of methyl propionate over a Pd(1 1 1) catalyst model. Journal of Catalysis, 2016, 333, 171-183.	6.2	37
50	Adaptive-Partitioning QM/MM Dynamics Simulations: 3. Solvent Molecules Entering and Leaving Protein Binding Sites. Journal of Chemical Theory and Computation, 2014, 10, 4765-4776.	5.3	36
51	Direct Oxidation of Methane to Methanol Enabled by Electronic Atomic Monolayer–Metal Support Interaction. ACS Catalysis, 2019, 9, 6073-6079.	11.2	36
52	Ethylene glycol reforming on Pt(111): first-principles microkinetic modeling in vapor and aqueous phases. Catalysis Science and Technology, 2016, 6, 8242-8256.	4.1	35
53	Nature of Pt <sub><i>n</i></sub> /CeO <sub>2</sub> (111) Surface under Water–Gas Shift Reaction Conditions: A Constrained ab Initio Thermodynamics Study. Journal of Physical Chemistry C, 2012, 116, 9029-9042.	3.1	34
54	Understanding Active Sites in the Water–Gas Shift Reaction for Pt–Re Catalysts on Titania. ACS Catalysis, 2017, 7, 2597-2606.	11.2	34

#	Article	IF	CITATIONS
55	Study of molecular shape and non-ideality effects on mixture adsorption isotherms of small molecules in carbon nanotubes: A grand canonical Monte Carlo simulation study. Chemical Engineering Science, 2002, 57, 2439-2448.	3.8	31
56	Nucleation, Growth, and Adsorbate-Induced Changes in Composition for Co–Au Bimetallic Clusters on TiO <sub>2</sub> . Journal of Physical Chemistry C, 2012, 116, 24616-24629.	3.1	31
57	Investigation of solvent effects on the hydrodeoxygenation of guaiacol over Ru catalysts. Catalysis Science and Technology, 2019, 9, 6253-6273.	4.1	28
58	Solving the equations of motion for mixed atomistic and coarse-grained systems. Molecular Simulation, 2009, 35, 962-973.	2.0	27
59	Hydrodeoxygenation of propanoic acid over silica-supported palladium: effect of metal particle size. Catalysis Science and Technology, 2014, 4, 3909-3916.	4.1	25
60	Microkinetic analysis of C3–C5 ketone hydrogenation over supported Ru catalysts. Journal of Catalysis, 2017, 348, 59-74.	6.2	24
61	Mechanistic study of the ceria supported, re-catalyzed deoxydehydration of vicinal OH groups. Catalysis Science and Technology, 2018, 8, 5750-5762.	4.1	24
62	A Multiple Filter Based Neural Network Approach to the Extrapolation of Adsorption Energies on Metal Surfaces for Catalysis Applications. Journal of Chemical Theory and Computation, 2020, 16, 1105-1114.	5.3	24
63	Mechanism of Sulfur Poisoning of Sr <sub>2</sub> Fe <sub>1.5</sub> Mo <sub>0.5</sub> O <sub>6-î´</sub> Perovskite Anode under Solid Oxide Fuel Cell Conditions. Journal of Physical Chemistry C, 2014, 118, 23545-23552.	3.1	23
64	Titaniaâ€Supported Singleâ€Atom Platinum Catalyst for Waterâ€Gas Shift Reaction. Chemie-Ingenieur-Technik, 2017, 89, 1343-1349.	0.8	22
65	Microkinetic analysis of acetone hydrogenation over Pt/SiO2. Journal of Catalysis, 2019, 374, 183-198.	6.2	22
66	Importance of Angelica Lactone Formation in the Hydrodeoxygenation of Levulinic Acid to γ-Valerolactone over a Ru(0001) Model Surface. Journal of Physical Chemistry C, 2017, 121, 18746-18761.	3.1	21
67	Computational Investigation of Aqueous Phase Effects on the Dehydrogenation and Dehydroxylation of Polyols over Pt(111). Journal of Physical Chemistry C, 2019, 123, 19052-19065.	3.1	21
68	Prediction of Transition-State Energies of Hydrodeoxygenation Reactions on Transition-Metal Surfaces Based on Machine Learning. Journal of Physical Chemistry C, 2019, 123, 29804-29810.	3.1	21
69	Enhanced reducibility and conductivity of Na/K-doped SrTi0.8Nb0.2O3. Journal of Materials Chemistry A, 2013, 1, 10546.	10.3	20
70	Effect of Palladium Surface Structure on the Hydrodeoxygenation of Propanoic Acid: Identification of Active Sites. Journal of Physical Chemistry C, 2015, 119, 1928-1942.	3.1	20
71	<i>In Situ</i> Ambient Pressure X-ray Photoelectron Spectroscopy Studies of Methanol Oxidation on Pt(111) and Pt–Re Alloys. Journal of Physical Chemistry C, 2015, 119, 23082-23093.	3.1	20
72	Obtaining mixed ionic/electronic conductivity in perovskite oxides in a reducing environment: A computational prediction for doped SrTiO3. Solid State Ionics, 2012, 228, 37-45.	2.7	19

#	Article	IF	CITATIONS
73	Rational design of mixed ionic and electronic conducting perovskite oxides for solid oxide fuel cell anode materials: A case study for doped SrTiO3. Journal of Power Sources, 2014, 245, 875-885.	7.8	19
74	Investigation of the high-temperature redox chemistry of Sr <sub>2</sub> Fe <sub>1.5</sub> Mo <sub>0.5</sub> O <sub>6â^î(</sub> via in situ neutron diffraction. Journal of Materials Chemistry A, 2014, 2, 4045-4054.	10.3	19
75	Theoretical investigation of the hydrodeoxygenation of methyl propionate over Pd (111) model surfaces Catalysis Science and Technology 2014, 4, 3981-3992. Density functional theory study on the electronic structure of mini:math	4.1	18
76	xmlns:mml="http://www.w3.org/1998/Math/MathML" display="inline"> <mml:mi>n</mml:mi> - and <mml:math <br="" xmlns:mml="http://www.w3.org/1998/Math/MathML">display="inline"&gt;<mml:mi>p</mml:mi></mml:math> -type doped SrTiO <mml:math xmlns:mml="http://www.3.org/1998/Math/MathML" display="inline"&gt;<mml:msub><mml:mrow< td=""><td>3.2</td><td>16</td></mml:mrow<></mml:msub></mml:math 	3.2	16
77	/> <mml:mn>3</mml:mn> at anodic solid oxide fuel cell conditions. Physical ②ptimum Reaction Conditions for 1,4-Anhydroerythritol and Xylitol Hydrodeoxygenation over a ReO <sub><i>x</i></sub> –Pd/CeO <sub>2</sub> Catalyst via Design of Experiments. Industrial & Engineering Chemistry Research, 2019, 58, 8681-8689.	3.7	16
78	Dependency of solvation effects on metal identity in surface reactions. Communications Chemistry, 2020, 3, .	4.5	15
79	Propane Dehydrogenation on Platinum Catalysts: Identifying the Active Sites through Bayesian Analysis. ACS Catalysis, 2022, 12, 2487-2498.	11.2	15
80	Unraveling the mechanism of the hydrodeoxygenation of propionic acid over a Pt (1Â1Â1) surface in vapor and liquid phases. Journal of Catalysis, 2020, 381, 547-560.	6.2	14
81	Reaction kinetics of the electrochemical oxidation of CO and syngas fuels on a Sr <sub>2</sub> Fe <sub>1.5</sub> Mo <sub>0.5</sub> O <sub>6ā^δ</sub> perovskite anode. Journal of Materials Chemistry A, 2015, 3, 21618-21629.	10.3	13
82	Deoxydehydration of 1,4-anhydroerythritol over anatase TiO <sub>2</sub> (101)-supported ReO <sub>x</sub> and MoO <sub>x</sub> . Catalysis Science and Technology, 2020, 10, 3731-3738.	4.1	13
83	Unraveling the mechanism of propanoic acid hydrodeoxygenation on palladium using deuterium kinetic isotope effects. Journal of Molecular Catalysis A, 2015, 406, 85-93.	4.8	12
84	Understanding the effect of Mo2C support on the activity of Cu for the hydrodeoxygenation of glycerol. Journal of Catalysis, 2020, 388, 141-153.	6.2	12
85	Supported Bifunctional Molybdenum Oxide-Palladium Catalysts for Selective Hydrodeoxygenation of Biomass-Derived Polyols and 1,4-Anhydroerythritol. ACS Sustainable Chemistry and Engineering, 2022, 10, 5719-5727.	6.7	12
86	In-Situ Oxygen Isotopic Exchange Vibrational Spectroscopy of Rhenium Oxide Surface Structures on Cerium Oxide. Journal of Physical Chemistry C, 2020, 124, 7174-7181.	3.1	11
87	Kinetics Study of the Hydrodeoxygenation of Xylitol over a ReOx-Pd/CeO2 Catalyst. Catalysts, 2021, 11, 108.	3.5	11
88	Highly Efficient Deoxydehydration and Hydrodeoxygenation on MoS <sub>2</sub> -Supported Transition-Metal Atoms through a C–H Activation Mechanism. ACS Catalysis, 2020, 10, 11346-11355.	11.2	10
89	Theoretical Investigation of Solvent Effects on the Hydrodeoxygenation of Propionic Acid over a Ni(111) Catalyst Model. Journal of Physical Chemistry C, 2020, 124, 16488-16500.	3.1	10
90	Oxidative dehydrogenation of propane on the oxygen adsorbed edges of boron nitride nanoribbons. Catalysis Science and Technology, 2020, 10, 5181-5195.	4.1	10

#	Article	IF	CITATIONS
91	Comparative Study on the Machine Learning-Based Prediction of Adsorption Energies for Ring and Chain Species on Metal Catalyst Surfaces. Journal of Physical Chemistry C, 2021, 125, 17742-17748.	3.1	10
92	Unraveling Unique Surface Chemistry of Transition Metal Nitrides in Controlling Selective C–O Bond Scission Pathways of Glycerol. Jacs Au, 2022, 2, 367-379.	7.9	10
93	Tight-Binding Configuration Interaction (TBCI): A Noniterative Approach to Incorporating Electrostatics into Tight Binding. Journal of Chemical Theory and Computation, 2008, 4, 804-818.	5.3	9
94	Investigation of the reaction mechanism of the hydrodeoxygenation of propionic acid over a Rh(1 1 1) surface: A first principles study. Journal of Catalysis, 2020, 391, 98-110.	6.2	8
95	Preferential Oxidation of CO in Hydrogen at Nonmetal Active Sites with High Activity and Selectivity. ACS Catalysis, 2020, 10, 5362-5370.	11.2	8
96	Probing surface-adsorbate interactions through active particle dynamics. Journal of Colloid and Interface Science, 2022, 614, 425-435.	9.4	7
97	Selective activation of methane C H bond in the presence of methanol. Journal of Catalysis, 2020, 386, 12-18.	6.2	6
98	An ab initio study of the oxygen defect formation and oxide ion migration in (Sr1-xPrx)2FeO4±δ. Journal of Power Sources, 2021, 515, 230602.	7.8	5
99	Surface structure sensitivity of hydrodeoxygenation of biomass-derived organic acids over palladium catalysts: a microkinetic modeling approach. Catalysis Science and Technology, 2021, 11, 6163-6181.	4.1	4
100	Dilute Limit Alloy Pd–Cu Bimetallic Catalysts Prepared by Simultaneous Strong Electrostatic Adsorption: A Combined Infrared Spectroscopic and Density Functional Theory Investigation. Journal of Physical Chemistry C, 2022, 126, 11111-11128.	3.1	4
101	Computational Investigation of the Catalytic Hydrodeoxygenation of Propanoic Acid over a Cu(111) Surface. Journal of Physical Chemistry C, 2021, 125, 19276-19293.	3.1	3
102	Kinetic modeling of nitrous oxide decomposition on Fe-ZSM-5 in the presence of nitric oxide based on parameters obtained from first-principles calculations. Catalysis Science and Technology, 2021, 11, 3539-3555.	4.1	3
103	Aqueous-phase effects on ethanol decomposition over Ru-based catalysts. Catalysis Science and Technology, 2021, 11, 6695-6707.	4.1	2
104	Kinetic and Mechanistic Analysis of the Hydrodeoxygenation of Propanoic Acid on Pt/SiO <sub>2</sub> . Industrial & Engineering Chemistry Research, 2021, 60, 16171-16187.	3.7	2
105	Understanding Selective Hydrodeoxygenation of 1,2- and 1,3-Propanediols on Cu/Mo <sub>2</sub> C via Multiscale Modeling. ACS Catalysis, 2022, 12, 4581-4596.	11.2	2
106	Comprehensive DFT Study of Nitrous Oxide Decomposition over Fe-ZSM-5 ChemInform, 2005, 36, no.	0.0	0